

Structural origin of the mobility enhancement in a pentacene thin-film transistor with a photocrosslinking insulator

Jin-Hyuk Bae, Won-Ho Kim, Hyeok Kim, Changhee Lee, and Sin-Doo Lee^{a)}
*School of Electrical Engineering No. 32, Seoul National University, Kwanak P. O. Box 34,
 Seoul 151-600, Korea*

(Received 28 May 2007; accepted 25 July 2007; published online 19 September 2007)

We present the underlying mechanism for the mobility enhancement in a pentacene thin-film transistor (TFT) with a photocrosslinking polymeric insulator, poly(vinyl cinnamate) (PVCi). Experimental results for the optical anisotropy, x-ray diffraction, and microscopic layer-by-layer coverage of the pentacene film on the photocrosslinked PVCi layer, exposed to a linearly polarized ultraviolet (LPUV) light, clearly demonstrate the importance of the structural packing of pentacene grains rather than the directional alignment of the pentacene molecules for the mobility enhancement. The packing density of pentacene grains is directly related to the number of photocrosslinking sites of the PVCi insulator produced by the LPUV. It is found that the mobility in the pentacene TFT is linearly proportional to the number of photocrosslinked sites of the PVCi insulator serving as interaction sites for the layer-by-layer coverage of the pentacene molecules with no preferred orientation. © 2007 American Institute of Physics. [DOI: 10.1063/1.2780869]

I. INTRODUCTION

An exciting prospect in plastic electronics lies in the development of reliable, high-performance organic thin-film transistors (OTFTs) that are applicable for flexible displays, smart cards, and a variety of sensors.¹⁻³ It is believed that the carrier mobility, which is one of the most important factors dictating the electrical performances of the OTFTs, depends strongly on the interfacial interactions between an organic semiconductor and a gate insulator. For instance, the mobility in a pentacene TFT with an inorganic SiO₂ insulator was found to be 1.6 cm²/V s (Ref. 4) while that in a pentacene TFT with a nontreated polymeric insulator was about 0.3 cm²/V s.⁵ For a phototreated polyimide insulator, it was reported that the mobility reaches as high as 0.7 cm²/V s due to the directional alignment of pentacene molecules.⁶ More recently, it has been demonstrated that the solvent processing temperature of a polymeric insulator significantly alters the interfacial interactions that play a critical role on the structural arrangement of the pentacene molecules.⁷ Measurements of the peak intensities and the peak positions of the x-ray diffraction (XRD) patterns in addition to the surface morphologies showed the directional ordering and the physical state of the pentacene molecules.⁸⁻¹⁰ However, the underlying physics behind the charge transport associated with the interfacial phenomena in the OTFTs has not been fully understood so far. Since the growth morphology of organic semiconducting molecules is primarily governed by the physicochemical interactions at an interface of a gate insulator, it is extremely important to explore the underlying mechanism for the growth morphology in terms of the interfacial interactions, producing the mobility enhancement

through the structural packing and/or the directional alignment of the constituent molecules, from both scientific and technological viewpoints.

In this work, we present the physical origin of the mobility enhancement in a pentacene TFT with a photocrosslinking polymeric gate insulator, poly(vinyl cinnamate) (PVCi), which is known to align liquid crystals (LCs) when exposed to a linearly polarized ultraviolet (LPUV) light.¹¹ Our experimental results for the optical anisotropy, the XRD, and the layer-by-layer coverage of the pentacene film revealed that the mobility enhancement results mainly from the dense growth morphology due to the structural packing of the pentacene grains rather than the directional alignment of the pentacene molecules on the LPUV exposed PVCi insulator. The mobility in the pentacene TFT is linearly proportional to the number of the photocrosslinked sites of the LPUV exposed PVCi layer that act as the interaction sites for the layer-by-layer coverage of the pentacene molecules with no preferred orientation. No considerable difference between the mobilities along two directions of the current flow, perpendicular and parallel to the LPUV polarization, was observed. This implies that the increase in the packing density of the pentacene grains on a gate insulator plays a more critical role in the mobility enhancement than the directional alignment of the pentacene molecules. In Sec. II, we describe the pentacene film preparation and the optical, structural, and morphological measurements. Experimental results for the optical anisotropy, the XRD, and the layer-by-layer coverage of the pentacene film on the PVCi insulator are presented in Sec. III. In Sec. IV, the electrical properties of the pentacene TFTs are presented. Some concluding remarks are made in Sec. V.

II. EXPERIMENTAL CONSIDERATION

A top-contact, bottom gate pentacene TFT structure with the PVCi insulator, shown in Fig. 1(a), was used in our study.

^{a)}Author to whom correspondence should be addressed. Electronic mail: sidlee@plaza.snu.ac.kr

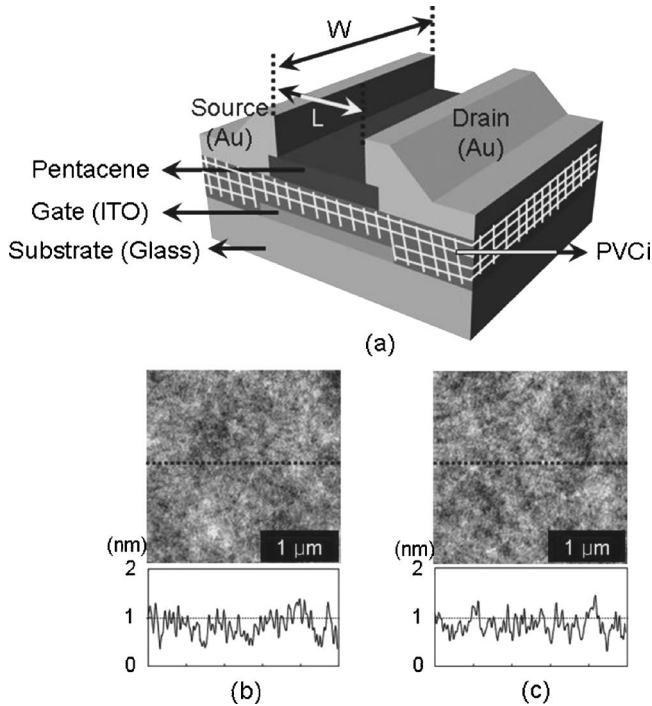


FIG. 1. (a) Our top-contact, bottom gate pentacene TFT. The SPM images and the morphological profiles of the PVCi layer (b) without the LPUV exposure and (c) with the LPUV exposure for 180 s. Morphological profiles were obtained along the black dotted lines in the SPM images.

The indium-tin-oxide (ITO) was used for the gate electrode. The ITO patterned glass substrate was cleaned up with acetone, isopropylalcohol, methanol, and de-ionized water in sequence. The PVCi (Sigma-Aldrich, Ltd.), dissolved in cyclopentanone in 10 wt %, was spin coated and cured at 60 °C for 5 h to remove any residual solvent, cyclopentanone.⁷ The thickness and the capacitance per unit area of the PVCi layer were measured as 570 nm and 5.9 nF/cm², respectively. The photocrosslinking reaction¹² in the PVCi layer was produced using a broadband UV light source. The LPUV light was exposed onto the PVCi layer for 180 s at the intensity of 10 mW/cm². It is known that the crosslinking density is proportional to the optical anisotropy induced in the PVCi layer.¹³ The phase retardation of the PVCi layer was measured using a photoelastic modulation (PEM) method with a He-Ne laser at the wavelength λ of 633 nm.¹⁴ For preparing an active layer in the OTFT, the pentacene molecules were deposited on the top of the PVCi insulator at the rate of 0.5 Å/s under the pressure of about 10⁻⁶ Torr. The pentacene material, purchased from Sigma-Aldrich, Ltd., was used without further purification. The pentacene film thickness was measured as 60 nm. The source electrode and the drain electrode were prepared on the pentacene film using gold (Au) at the deposition rate of 1 Å/s. The thickness of Au was 80 nm. The length and the width of the channel were 50 μ m and 1 mm, respectively. The electrical measurements of the fabricated pentacene TFTs were performed using a semiconductor parameter analyzer (HP 4155A) under ambient pressure at room temperature. The XRD measurements were carried out using a diffractometer (D8 DISCOVER, Bruker Co., Ltd.) with graphite monochromatized Cu K_{α} radiation ($\lambda=1.54$ Å). The surface mor-

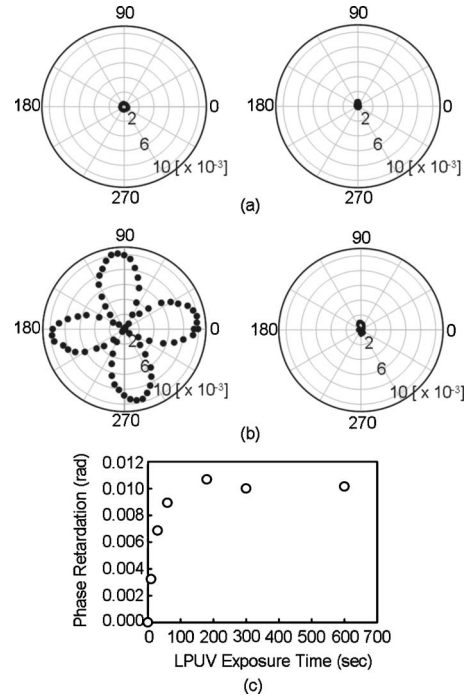


FIG. 2. (a) The phase retardation of the bare PVCi layer and that of the pentacene layer itself deposited on it, (b) the phase retardation of the LPUV exposed PVCi layer for 180 s and that of the pentacene layer itself deposited on it, and (c) the phase retardation of the PVCi layer as a function of the LPUV exposure time. The right column in (a) and (b) shows the phase retardation of the pentacene layer itself having no directional alignment.

phologies of both the PVCi layer and the pentacene film were examined by an atomic scanning probe microscope (SPM) (SPA 400, Seiko Instruments Co., Ltd.). The cantilevers of the SPM were used in the tapping mode. The grain size and the surface roughness were determined from the SPM data scanned in the area of 2.5 μ m \times 2.5 μ m.

III. CHARACTERIZATION OF THE PVCi AND PENTACENE THIN FILMS

A. Optical anisotropy

We first examine the surface properties of the PVCi insulator layers upon the LPUV exposure and the resulting structural arrangement of the pentacene molecules deposited on them. As shown in Figs. 1(b) and 1(c), the surface roughness of a bare PVCi layer and that of a photocrosslinked PVCi layer by the LPUV exposure for 180 s were nearly same as 2.5 \pm 0.2 Å. Therefore, the effect of the surface roughness of the PVCi insulator on the growth morphology of the pentacene film is negligible unlike in a previous study.¹⁵ Generally, it is believed that one of the significant factors influencing the charge transport in the pentacene film is the directional ordering of the pentacene molecules which produce nonzero optical anisotropy. More specifically, a preferred orientation of the elongated pentacene molecules results in the optical anisotropy. The phase retardation of the bare PVCi and that of the LPUV exposed, photocrosslinked PVCi, measured using the PEM method, are shown in the left column of Figs. 2(a) and 2(b), respectively.

The PVCi undergoes an anisotropic photocrosslinking reaction upon the LPUV exposure. The photochemical reac-

tion of a cinnamate polymer is generally induced by the reaction of the carbon double bonds of cinnamate sidegroups under the UV irradiation. The irradiation of the LPUV breaks the C=C bonds of cinnamate side chains that are parallel to the direction of the LPUV. The broken sidechains adjacent to main chains cause [2+2] cycloaddition and then create an anisotropic distribution of cross-linked molecules along the direction perpendicular to the LPUV.¹² The LPUV produces the orientational ordering of the molecules along the direction perpendicular to the LPUV. This gives an optical anisotropy of the PVCi layer by such photocrosslinking reaction.

As shown in the left column of Fig. 2, it is clear that the LPUV exposed PVCi layer of 570 nm shows nonzero optical anisotropy while the bare PVCi layer exhibits no optical anisotropy. The phase retardation of the pentacene film of 60 nm on the bare PVCi and that on the LPUV exposed PVCi are shown in the right column of Figs. 2(a) and 2(b). Interestingly, the two pentacene films deposited on the bare PVCi and the LPUV exposed PVCi exhibit no optical anisotropy (or no directional order) within our optical resolution although the LPUV exposed PVCi layer itself has a finite optical anisotropy (about 0.01 rad) as shown in the left column of Fig. 2.

From the fact that the phase retardation shows axial symmetry, i.e., no anisotropy, it was found that in contrast to the LC molecules,¹¹ the pentacene molecules may not be substantially aligned on the LPUV exposed PVCi layer along a certain direction. This means that no ordered and/or crystalline state of the pentacene molecules on the LPUV exposed PVCi layer would be produced. A more detailed description of the structural order of the pentacene molecules will be given in the following section where the XRD results are presented. The measured phase retardation (or the optical anisotropy) of the PVCi layer is monitored as a function of the LPUV exposure time. As shown in Fig. 2(c), the measured values of the phase retardation increase monotonically and become saturated at about 0.01 rad with increasing the LPUV exposure time. In fact, the PVCi molecules were fully aligned and photocrosslinked after 180 s of the LPUV exposure. No further crosslinks were observed above the LPUV exposure for 180 s. Since the optical anisotropy is proportional to the photocrosslinked density,¹³ the interaction sites for the pentacene molecules at the PVCi interface increase with increasing the optical anisotropy of the PVCi layer.

B. X-ray diffraction

We now discuss the XRD data for the pentacene films (all 60 nm) on both the bare PVCi layer and the photocrosslinked PVCi layer upon the LPUV exposure. From the XRD data, the change in the structural arrangement of the pentacene molecules, the crystallinity and/or the directional order, can be determined as in previous works.⁸⁻¹⁰ It has been argued that the intensity increase in the XRD patterns indicates the presence of a more ordered state of pentacene molecules. As an example, the enhancement of the XRD intensity in a pentacene film on a rubbed self-assembling monolayer represents a certain degree of the crystallinity of the pentacene film.¹⁰ As shown in Figs. 3(a) and 3(b), in our

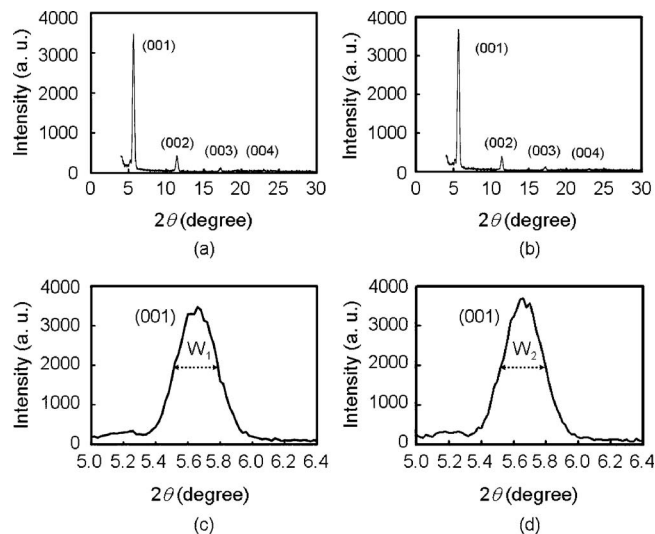


FIG. 3. X-ray diffraction results for a pentacene film of 60 nm thick grown on (a) the bare PVCi layer and (b) the LPUV exposed PVCi layer for 180 s. The corresponding FWHMs, W_1 and W_2 , of the first order diffraction peaks in (001) are shown in (c) and (d).

case, the XRD intensities of the pentacene films on the bare PVCi and the LPUV exposed PVCi show essentially no difference. Moreover, the full width at half maximum (FWHM), W_1 or W_2 , of the first order XRD peak in (001) remains unchanged as clearly shown in Figs. 3(c) and 3(d). It is then concluded that the directional order of the pentacene molecules is negligible and the crystallite (grain) size in the pentacene film remains nearly same.^{16,17} This is in agreement with our SPM observation of the grain size in the pentacene films of 60 nm thick on both the bare PVCi layer and the LPUV exposed PVCi layer.

Based on the first order diffraction peak at 5.7° in our XRD data, it was found that the layer spacing of pentacene molecules, d_{001} , is 1.54 nm. This is consistent with previous results.¹⁸⁻²⁰ It is interesting to note that the measured d_{001} is somewhat smaller than the length of a single pentacene molecule (1.60 nm). This suggests that the long axes of the pentacene molecules are slightly tilted.¹⁹

C. Surface morphology

Let us determine how the interfacial interaction sites at the PVCi insulator influence the growth morphology of the pentacene film upon the LPUV exposure. The layer-by-layer growth of the pentacene molecules on two different PVCi insulator layers, one of which was a bare PVCi layer and the other was the LPUV exposed PVCi layer for 180 s, was carried out. It should be noted that no difference in the surface roughness between the two PVCi layers was observed. It is evident from Figs. 4(a) and 4(b) that the nucleation sites for the pentacene grains on the LPUV exposed PVCi layer become dense from the initial growth stage. For the nominal thickness of 4 Å, the monolayer coverage of the pentacene grains on the LPUV exposed PVCi is about 35% higher than that on the bare PVCi. This results from the presence of more nucleation sites produced during the photocrosslinking reaction of the PVCi molecules upon the LPUV exposure. Note that ultrathin molecular layers next to a dielectric interface

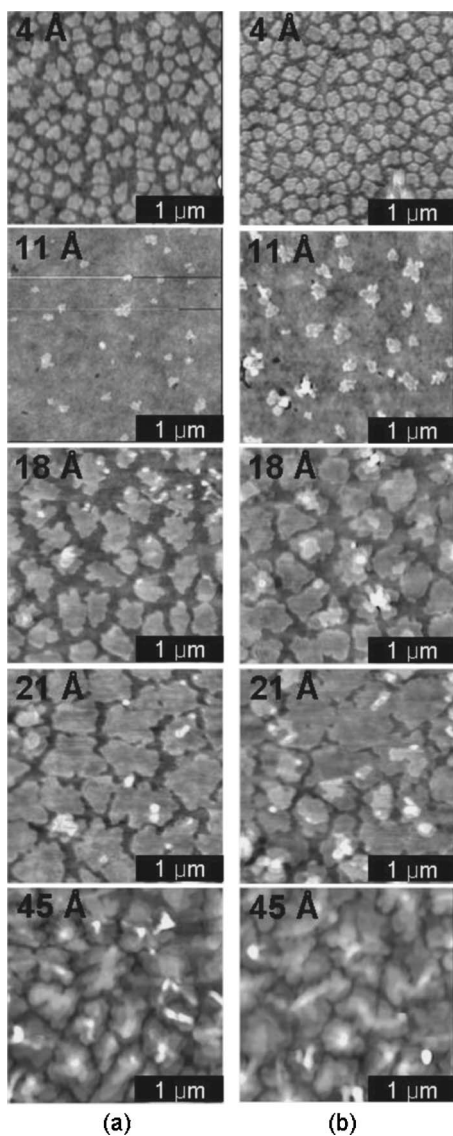


FIG. 4. The SPM images of the layer-by-layer growth of the pentacene film (a) on the bare PVCi layer and (b) on the LPUV exposed PVCi layer for 180 s. The nominal thickness of each pentacene film is 4, 11, 18, 21, and 45 Å.

were found to dominate the charge transport in an organic semiconductor.²¹ The full coverage of the first pentacene film became completed for the nominal thickness of about 11 Å as shown in Figs. 4(a) and 4(b). As the pentacene film thickness increases, the layer-by-layer coverage proceeds in a step of about 11 Å, which is somewhat less than the length (16 Å) of a single pentacene molecule. Under this circumstance, the pentacene molecules are considered to be slightly tilted away from the surface normal of the PVCi layer. This agrees well with the XRD data. Above the nominal thickness of 45 Å, corresponding to about four stacked pentacene layers, no microscopic difference between the pentacene film on the LPUV exposed PVCi and that on the bare PVCi was observed.

This layer-by-layer growth of the pentacene film in the Stransky–Krastanov mode,^{22,23} observed in our case, is expected to play a key role on the charge transport in the pentacene TFT. Considering that the grain sizes in the pentacene films of 60 nm thick are essentially unchanged as discussed

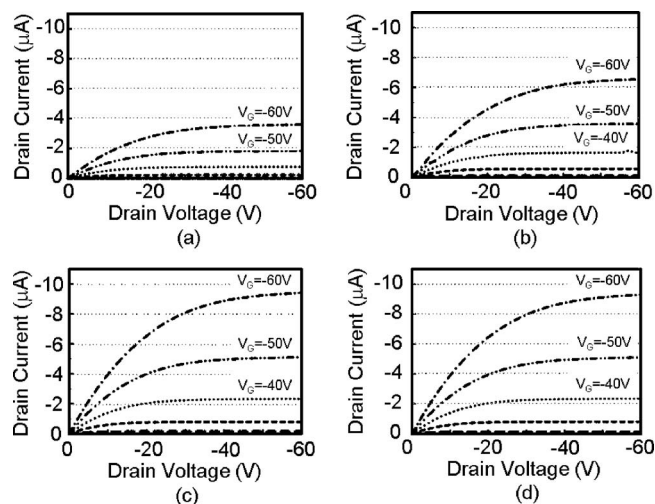


FIG. 5. The output characteristic curves of our four pentacene TFTs with four different PVCi insulator layers, exposed to the LPUV for (a) 0, (b) 30, (c) 180, and (d) 600 s.

in our XRD data, the morphological growth in the initial stage is extremely important for the charge transport in the pentacene film. Therefore, the mobility enhancement in the OTFT should be understood in terms of the structural packing of the grains within the framework of the initial layer-by-layer coverage instead of many stacked molecular layers.²⁰ In addition, the presence of grain boundaries will significantly limit the transport of charges, i.e., the carrier mobility. More photocrosslinked sites on the LPUV exposed PVCi layer give more nucleation sites for the pentacene grains at the PVCi insulator interface as shown in Fig. 4(b). It should be emphasized that from the optical anisotropy results, the XRD data, and the layer-by-layer coverage, the dense growth morphology in the pentacene film on the LPUV exposed PVCi layer is attributed to the high packing of the pentacene grains rather than the alignment of the pentacene molecules along a preferred direction. In other words, the LPUV exposure on the PVCi layer produces layer-by-layer packing of the pentacene grains without directional alignment of the pentacene molecules at photocrosslinked sites.

IV. ELECTRICAL PROPERTIES OF PENTACENE TFTS

Based on the earlier results, we now describe the physical mechanism for the mobility enhancement in view of the difference in the charge transport between two types of the pentacene TFTs having four different PVCi layers, one of which is a bare (or isotropic) PVCi and the other three photocrosslinked PVCis upon the LPUV exposure for 30, 180, and 600 s. Note that all the four PVCi insulators exhibit essentially no morphological difference. The output characteristic curves of our four pentacene TFTs are shown in Fig. 5. Among the four OTFTs, one with the isotropic PVCi shown in Fig. 5(a) has the lowest drain current for given drain and gate voltages. As the LPUV exposure time increases from 0 to 600 s, the drain current of the OTFT in the saturation region increases from -3.59 up to -9.40 μA and becomes saturated above 180 s on moving from Figs.

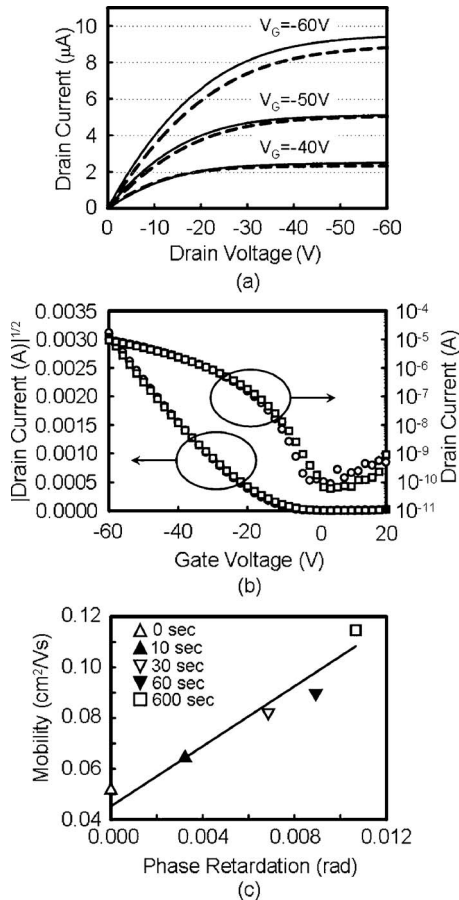


FIG. 6. (a) The output characteristic curves measured along two directions of the current flow, perpendicular (denoted by a solid line) and parallel (denoted by a dashed line) to the LPUV polarization, (b) the corresponding transfer characteristic curves perpendicular (represented by open circles) and parallel to (represented by open squares) the LPUV polarization, and (c) the mobility in the pentacene TFT as a function of the phase retardation of the LPUV exposed PVCi layer. The solid line represents a linear fit.

5(a)–5(d). The threshold voltage of -20 V and the current on-off ratio of 10^5 remain almost same in the four OTFTs we studied. In the saturation regime, the mobility of the OTFT is calculated using the following equation:²⁴

$$I_D = \frac{W}{2L} C_i \mu_{\text{sat}} (V_G - V_T)^2, \quad (1)$$

where I_D is the drain current, L and W are the channel length and the channel width, respectively, C_i is the insulator capacitance per unit area, μ_{sat} is the carrier mobility in the saturation region, V_G is the gate bias voltage, and V_T is the threshold voltage. The carrier mobility in the saturation region upon the LPUV exposure from 0 to 600 s were found to show a reminiscent behavior of the phase retardation as shown in Fig. 2(c), ranging from 0.05 to 0.12 $\text{cm}^2/\text{V s}$ with increasing the LPUV exposure time.

As another direct evidence of supporting that the mobility enhancement results primarily from the high packing of the pentacene grains rather than the directional alignment of the pentacene molecules, the output and transfer characteristic curves measured along two directions of the current flow, perpendicular and parallel to the LPUV polarization, are presented in Figs. 6(a) and 6(b). Clearly, no substantial differ-

ence (about 10%) between the two directions was observed. The longitudinal mobility μ_{\parallel} and the transverse mobility μ_{\perp} to the polarization of the LPUV, determined from the transfer characteristic curves in Fig. 6(b), were given as $\mu_{\perp} \approx 1.12\mu_{\parallel}$ with $\mu_{\parallel} = 0.09 \text{ cm}^2/\text{V s}$. The relationship between the mobility in the pentacene TFT and the phase retardation (or the optical anisotropy) of the LPUV exposed PVCi insulator is shown in Fig. 6(c). The linear relationship tells us that the mobility is directly proportional to the number of the photocrosslinked sites or the nucleation sites in the PVCi layer that provide the high packing of the pentacene grains with no directional alignment of pentacene molecules.

V. CONCLUDING REMARKS

We presented a rather complete picture of the underlying mechanism for the mobility enhancement in a pentacene TFT with a photocrosslinking polymer insulator within the framework of the initial layer-by-layer coverage of the pentacene molecules. From the optical anisotropy and the XRD measurements, it was found that in contrast to the LC molecules, no directional alignment of the pentacene molecules was produced on the LPUV exposed PVCi layer. Thus, the main physical origin of the mobility enhancement comes from the dense growth morphology of the pentacene molecules and grains at the photocrosslinked sites acting as the nucleation sites. The fact that no substantial difference was observed between the mobilities in two OTFTs, in one of which the current flow is parallel to the LPUV polarization and the other perpendicular to the LPUV polarization, definitely supports the importance of the high packing of pentacene grains rather than the directional alignment of pentacene molecules. The carrier mobility in the pentacene TFT with the LPUV exposed PVCi insulator was found to be linearly proportional to the optical anisotropy of the PVCi layer. For other crosslinking polymeric insulators, the mobilities will share the common features with the PVCi. The mobility of our OTFT on the PVCi would be much enhanced by the purification of the pentacene material and the moderation of the substrate heating used in the previous work.²⁵ This work is expected to provide at least a basis for developing promising polymer insulators to increase the carrier mobility in the OTFT.

ACKNOWLEDGMENTS

This work was supported in part by Samsung SDI-Seoul National University Display Innovation Program and by the Ministry of Science and Technology of Korea through the 21st Century Frontier Research and Development Program at the Information Display Center.

¹C. D. Dimitrakopoulos and P. R. L. Malenfant, *Adv. Mater.* (Weinheim, Ger.) **14**, 99 (2002).

²B. Crone, A. Dodabalapur, Y. Y. Lin, R. W. Filas, Z. Bao, A. Laduca, R. Sarpeshkar, H. E. Katz, and W. Li, *Nature* (London) **403**, 521 (2000).

³B. Crone, A. Dodabalapur, A. Gelperin, L. Torsi, H. E. Katz, A. J. Lovinger, and Z. Bao, *Appl. Phys. Lett.* **78**, 2229 (2001).

⁴M. Shtein, J. Mapel, J. B. Benziger, and S. R. Forrest, *Appl. Phys. Lett.* **81**, 268 (2002).

⁵Y. Kato, S. Iba, R. Teramoto, T. Sekitani, T. Someya, H. Kawaguchi, and T. Sakurai, *Appl. Phys. Lett.* **84**, 3789 (2004).

- ⁶W.-Y. Chou and H.-L. Cheng, *Adv. Funct. Mater.* **14**, 811 (2004).
- ⁷J.-H. Bae, J. Kim, W.-H. Kim, and S.-D. Lee, *Jpn. J. Appl. Phys., Part 1* **46**, 385 (2007).
- ⁸T. Komoda, Y. Endo, K. Kyuno, and A. Toriumi, *Jpn. J. Appl. Phys., Part 1* **41**, 2767 (2002).
- ⁹D. Guo, K. Sakamoto, K. Miki, S. Ikeda, and K. Saiki, *Appl. Phys. Lett.* **90**, 102117 (2007).
- ¹⁰S.-Z. Weng, W.-S. Hu, C.-H. Kuo, Y.-T. Tao, L.-J. Fan, and Y.-W. Yang, *Appl. Phys. Lett.* **89**, 172103 (2006).
- ¹¹M. Schadt, K. Schmitt, V. Kozinkov, and V. Chigrinov, *Jpn. J. Appl. Phys., Part 1* **31**, 2155 (1992).
- ¹²P. L. Egerton, E. Pitts, and A. Reiser, *Macromolecules* **14**, 95 (1981).
- ¹³I. Assaid, D. Bosc, and I. Hardy, *J. Phys. Chem. B* **108**, 2801 (2004).
- ¹⁴J.-H. Lee, C.-J. Yu, and S.-D. Lee, *Mol. Cryst. Liq. Cryst.* **321**, 317 (1998).
- ¹⁵S. Steudel, S. D. Vusser, S. D. Jonge, D. Janssen, S. Verlaak, J. Genoe, and P. Heremans, *Appl. Phys. Lett.* **85**, 4400 (2004).
- ¹⁶B. D. Cullity, *Elements of X-Ray Diffraction*, 2nd ed. (Addison-Wesley, Reading, MA, 1977), p. 102.
- ¹⁷D. Guo, S. Ikeda, K. Saiki, H. Miyazoe, and K. Terachima, *J. Appl. Phys.* **99**, 094502 (2006).
- ¹⁸S. D. Wang, X. Dong, C. S. Lee, and S. T. Lee, *J. Phys. Chem. B* **109**, 9892 (2005).
- ¹⁹C. D. Dimitrakopoulos, A. R. Brown, and A. Pomp, *J. Appl. Phys.* **80**, 2501 (1996).
- ²⁰W. Y. Chou, Y. S. Mai, H. L. Cheng, C. Y. Yeh, C. W. Kuo, F. C. Tang, D. Y. Shu, T. R. Yew, and T. C. Wen, *Org. Electron.* **7**, 445 (2006).
- ²¹F. Dinelli, M. Murgia, P. Levy, M. Cavallini, F. Biscarini, and D. M. de Leeuw, *Phys. Rev. Lett.* **92**, 116802 (2004).
- ²²R. Ruiz, A. Papadimitratos, A. C. Mayer, and G. G. Malliaras, *Adv. Mater. (Weinheim, Ger.)* **17**, 1795 (2005).
- ²³P. Parris, M. Passacantando, S. Picozzi, and L. Ottaviano, *Org. Electron.* **7**, 403 (2006).
- ²⁴C. D. Dimitrakopoulos and D. J. Mascaró, *IBM J. Res. Dev.* **45**, 11 (2001).
- ²⁵T. Cui and G. Liang, *Appl. Phys. Lett.* **86**, 064102 (2005).